

Numerical Analysis of Nano fluid on Stagnation Flow Past a stretching sheet in the Presence of Magneto hydrodynamics (MHD), Convective Heating in the presence of porous media

¹T.Rajeshwari

Department of Mathematical Sciences, N.T.R
Govt. degree college for women, Telangana, India

³K.Ramesh

Department of Mathematics, Sreenidhi Institute of Science
and Technology, Yamnampet, Ghatkesar, Madchal, T.S,
India

²S. Hari Singh Naik

Department of Mathematics, UCS, Osmania
University, Hyderabad, Telangana, 500007, India.

Abstract - In the present content an analysis is carried out to examine the effect of convective heat transfer on stagnation-point flow of Nano fluid towards a stretched sheet through porous medium in the presence of a magnetic field. Using suitable similarity transformations, the governing boundary-layer equations corresponding to the momentum, energy and concentration are reduced to non-linear ordinary differential equation. The transformed equations are then solved numerically using Keller Box method. The alterations in velocity, temperature and concentration for different values of physical parameters are plotted through graphs. An evaluation is made with previous results and we found a good similarity. Tables are used to analyse skin friction and the Nusselt and Sherwood values. The main findings of investigations are velocity increases as the increasing in velocity ratio parameter, porosity and decreases as increasing in magnetic parameter. The temperature profile increases with the enhancement in the values of Prandtl number and Bi finally concentration increases with the increasing values of Nt and Le and decreases with the increasing values of Brownian motion parameter.

Keywords— *Nanofluid, Porous media, Stagnation Flow, MHD, Convective Heating.*

INTRODUCTION

The thermal characteristics of base fluids could enhance by introduce the nanoparticles, the resultant fluids are called nanofluids. The nanofluids are homogeneous mixture of very small particles of size 10^{-9} m. Incorporation the

nanoparticles of metals (Al, Cu, Ag, etc.) or metal oxides (CuO, TiO₂, Al₂O₃, etc.) or nitride ceramics (AlN, Si₃N₄) or carbide ceramics (SiC, TiC), etc. to the based fluids like water, ethylene glycol, oil etc., the thermal conductivity is enhanced by an order of magnitude. The said nanofluids offer improved heat absorption, and also heat transfer rate as the specific heat of metal, it's based particles is very low as compared to water or other liquids. Nanofluids have potential applications in engineering and biomedical, etc. like in heat exchanger, refrigerators, microelectronics, engine cooling / vehicles thermal managements, hybrid-powered engines, coolants of nuclear reactor, cooling agent in airplanes, micro machines in micro reactors, automobiles, etc. Choi [1] introduced first time by usage of nanoparticles in base fluids and the results of experiments witnessed the thermal properties of fluids are enhanced through nanoparticles. Buongiorno group [2] developed a mathematical model, which exhibited the characteristic of thermophoresis and Brownian motion of nanoparticles. Later, many researchers used the nanofluids in various directions particularly for stretching sheets [3-6] cylinders [7-10] etc.

, Magneto-nanofluids have specific applications in biomedicine, optical modulators, magnetic cell separation, magneto-optical wavelength filters, silk float separation,

nonlinear optical materials, hyperthermia, optical switches, drug delivery, optical gratings etc. A magneto-nanofluid has both the liquid and magnetic properties. The used magnetic field influences the suspended particles and reorganizes their concentration in the fluid regime which powerfully influences the heat transfer analysis of the flow. Magneto-nanofluids are useful to guide the particles up the blood stream to a tumor with magnets. This is because the magnetic nanoparticles are regarded more adhesive to tumor cells than non-malignant cells. Such particles absorb more power than microparticles in alternating current magnetic fields tolerable in humans i.e., for cancer therapy. Several authors[11, 12, 13, 14] have discussed the MHD boundary layer flow, heat and mass transfer characteristics of nanofluids.

Motivating by above research work, the aim of this research work is to extend the research work of Ibrahim and Haq [15] and Ch.Janaiah and G.Upender Reddy [16] by excluding the effects Soret (Thermal diffusion) and Dufour (Diffusion thermo) on magnetohydrodynamic nanofluid flow towards a non-linear stretching sheet in presence of porous media, Thermophoresis, Brownian motion and Convective heating effects using numerical solutions.

The present research work is aims to study the effect of convective heat transfer on stagnation-point flow of nanofluid via a stretched sheet and porous medium in the presence of a magnetic field. Using suitable similarity transformations, the governing boundary-layer equations corresponding to the momentum, energy and concentration are reduced to non-linear ordinary differential equation. The transformed equations are then solved numerically by use of Keller-Box method. The alterations in velocity, temperature and concentration for different values of physical parameters are plotted. A comparison is made with the previous results and the results are found a good similarity. The evaluated skin-friction coefficients, Nusselt and Sherwood numbers are tabulated.

FORMULATION OF THE PROBLEM:

Consider a steady, laminar, incompressible electrically conducting, two dimensional flow of a nanofluid

past over a linear stretching surface in the direction of x -axes with the velocity $u_w(x) = ax$ where a is a constant, and y axis is normal to the sheet. A hot fluid with temperature T_f is applied to heat up or cool down the surface of the sheet at lower level by convective heat transfer mode, which provides the heat transfer coefficient h_f . A uniform magnetic field B_0 is applied in the transverse direction y normal to the surface and the induced magnetic field is assumed to be small compared to the applied magnetic field and so neglected. The ambient fluid temperature and Nano particles fraction have constant value T_∞ and C_∞ , respectively. Under the above conditions the physical coordinate system is shown in figure 1.

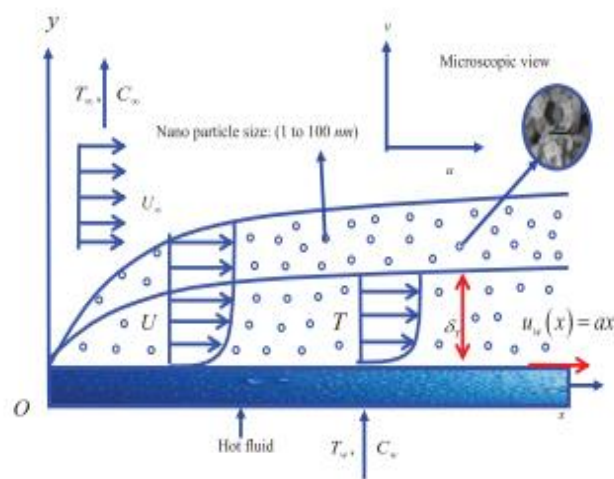


Figure-1: Geometry representation of the fluid

The governing equations [16] of the conservation of mass, momentum, energy and nanoparticle fraction is

$$u \frac{\partial u}{\partial x} + v \frac{\partial u}{\partial y} = \nu \frac{\partial^2 u}{\partial y^2} + U_\infty \frac{\partial U_\infty}{\partial x} - \left(\frac{\sigma B_0^2}{\rho_f} \right) (U_\infty - u) - \frac{\nu}{k_1} u \tag{1}$$

$$u \frac{\partial T}{\partial x} + v \frac{\partial T}{\partial y} = \alpha \frac{\partial^2 T}{\partial y^2} + \tau \left\{ D_B \left(\frac{\partial c}{\partial y} \frac{\partial T}{\partial y} \right) + \frac{D_T}{T_\infty} \left(\frac{\partial T}{\partial y} \right)^2 \right\} + \frac{D_m K_T}{c_s c_p} \frac{\partial^2 c}{\partial y^2} \tag{2}$$

$$\tag{3}$$

$$u \frac{\partial c}{\partial x} + v \frac{\partial c}{\partial y} = D_B \frac{\partial^2 c}{\partial y^2} + \frac{D_T}{T_\infty} \frac{\partial^2 T}{\partial y^2} + \frac{D_m K_T}{T_m} \frac{\partial^2 T}{\partial y^2}$$

(4)

The effect of the terms $\frac{D_m K_T}{C_\infty C_p} \frac{\partial^2 C}{\partial y^2}$, $\frac{D_m K_T}{T_m} \frac{\partial^2 T}{\partial y^2}$ in equation (3) and (4) are very negligible even though in the absence of these terms results obtained are in good agreement with the results obtained by Ch. Janaiah et al. [16].

$$\frac{\partial u}{\partial x} + \frac{\partial v}{\partial y} = 0$$

(5)

Momentum Equation

$$u \frac{\partial u}{\partial x} + v \frac{\partial u}{\partial y} = \nu \frac{\partial^2 u}{\partial y^2} + U_\infty \frac{\partial U_\infty}{\partial x} - \left(\frac{\sigma B_0^2}{\rho_f} \right) (U_\infty - u) - \frac{\nu}{k_1} u$$

(6)

Equation of Thermal Energy

$$u \frac{\partial T}{\partial x} + v \frac{\partial T}{\partial y} = \alpha \frac{\partial^2 T}{\partial y^2} + \tau \left\{ D_B \left(\frac{\partial c}{\partial y} \frac{\partial T}{\partial y} \right) + \frac{D_T}{T_\infty} \left(\frac{\partial T}{\partial y} \right)^2 \right\}$$

(7)

Equation of species Concentration

$$u \frac{\partial c}{\partial x} + v \frac{\partial c}{\partial y} = D_B \frac{\partial^2 c}{\partial y^2} + \frac{D_T}{T_\infty} \frac{\partial^2 T}{\partial y^2}$$

(8)

The Boundary Conditions for Nano Fluid flow are

$$u = u_w(x) = ax \text{ at } v = 0, \quad -k \frac{\partial T}{\partial y} = h_f(T_f - T), \quad D_B \frac{\partial c}{\partial y} + \frac{D_T}{T_\infty} \left(\frac{\partial T}{\partial y} \right) = 0 \text{ at } y = 0$$

$$u \rightarrow U_\infty = bx \text{ at } v = 0, \quad T \rightarrow T_\infty, C \rightarrow C_\infty \text{ as } y \rightarrow \infty$$

For solving equations (5) to (8) we introduced new transformations

$$\eta = y \sqrt{\frac{a}{\nu}}, \quad \psi = xf(\eta) \sqrt{a\nu}, \quad \theta = \frac{T-T_\infty}{T_f-T_\infty}, \quad \phi = \frac{c-C_\infty}{C_\infty}$$

(9)

Where $\psi(x, y)$ represents the Stream function and is defined by

$$u = \frac{\partial \psi}{\partial y} = \frac{\partial \psi}{\partial \eta} \frac{\partial \eta}{\partial y} = xf'(\eta) \sqrt{a\nu} \sqrt{\frac{a}{\nu}}$$

$$v = -\frac{\partial \psi}{\partial x} = -f(\eta) \sqrt{a\nu}$$

(10)

Using (9) the flow Eqs.(5) - (8) become

$$f''' + ff'' - f'^2 + A^2 + MA - (\lambda + M)f' = 0$$

(11)

$$\theta'' + Prf\theta' + PrNb\theta'\phi' + PrNt\theta'^2 = 0$$

$$Nb\phi'' + LeNbPrf\phi' + Nt\theta'' = 0$$

(12) (13)

Boundary Conditions

$$f = 0, f' = 1, \theta' = B_1(\theta - 1), \quad Nb\phi' + Nt\theta' = 0 \quad \text{as } \eta \rightarrow 0$$

$$f' = A, \theta \rightarrow 0, \phi \rightarrow 0 \quad \text{as } \eta \rightarrow \infty$$

(14)

Where the dimensionless parameters are

Velocity Ratio Parameter $A = \frac{b}{a}, Pr = \frac{\nu}{\alpha}, Nb = \frac{C_\infty \tau D_B}{\nu}, Nt = \frac{D_T}{T_\infty \nu} (T_f - T_\infty),$

porosity $\lambda = \frac{\nu}{ak_1},$ Magnetic field $M = -\left(\frac{\sigma B_0^2}{a\rho_f} \right)$

METHODOLOGY:

Stage 1: In the early stage, all ODEs must be converted to first-order ODEs. (11) - (13).

$$f' = p, p' = q, \theta' = t, \phi' = g$$

$$q' + fq - p^2 + A^2 + MA - (\lambda + M)p = 0$$

(15)

$$t' + Prft + PrNbtg + PrNt t^2 = 0$$

(16)

$$Nbg' + LeNbPrfg + Nt t' = 0$$

(17)

In order to solve the system of ordinary differential equations (11)–(13).The Following steps are used.

- Convert the system of ordinary differential equations into a set of equations of the first order.
- To solve ordinary differential equations, write the difference equations using the central differences.
- Using the Newton method, linearize the algebraic equations, and then write them down in matrix form.
- Use the block tridiagonal elimination method to solve the linear system. Substitute the above values in equations (15) - (17) and write the first order ODEs into finite differences by using $\frac{(f_j - f_{j-1})}{h_j} = \frac{(p_j - p_{j-1})}{2}$ transformation and linearize the difference Equations. numerical procedure

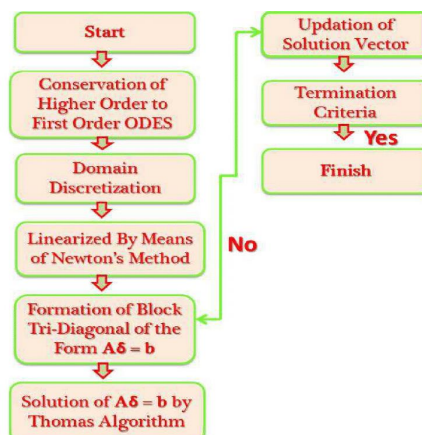


FIG-B: FLOW DIAGRAM OF THE KELLER BOX METHOD

The study investigated the momentum, energy, and concentration equation-governed non-Newtonian Nano fluid on Stagnation Flow Past a stretching sheet model, which is impacted by the Velocity ratio parameter, magnetic field, thermal radiation, , and chemical reaction. To solve the system of highly nonlinear ordinary differential equations, we use a Keller –Box Method. When fixing the values of $A, M, Nb, Bi, Le, Nt, \lambda, Pr$.

Fig.3 illustrates the variation in velocity with velocity ratio parameter A . Velocity ratio parameter is represents the relation of freestream velocity to stretching sheet velocity. An increase in A indicates the freestream velocity is higher than the stretching sheet velocity as a result impeding force acting on the fluid will decrease, and velocity increases. Fig.4 explains the effect of magnetic field on velocity. When the magnetic field's intensity is increased, a resistive Lorentz force is generated. The decrease in velocity profile is caused by this resistive force. Fig.5 shows how the Concentration profile is affected by the Brownian motion parameter Nb . The fluid molecules move randomly as the Brownian motion factor Nb rises, which causes an increase in the rate of fluid conversion and a decrease in concentration. Fig.6 examines the influence of Biot number Bi on temperature. The Biot number is a measure of how much thermal resistance there is for conduction inside a body compared to convection at the surface. As Biot number increases the resistance to conduction transmission is also increases, which causes the temperature at surface increase and thickness of thermal boundary layer also enhance.

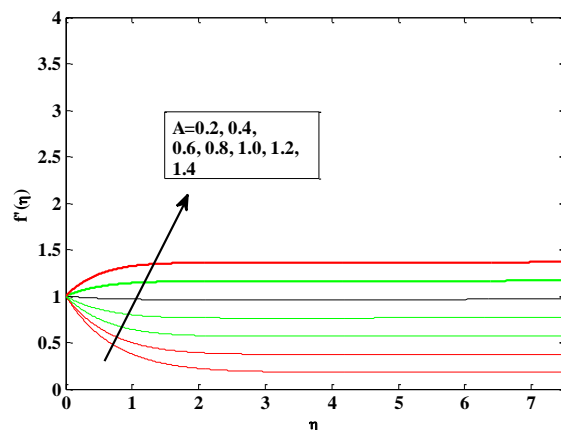


Figure-2: Effect of A on velocity

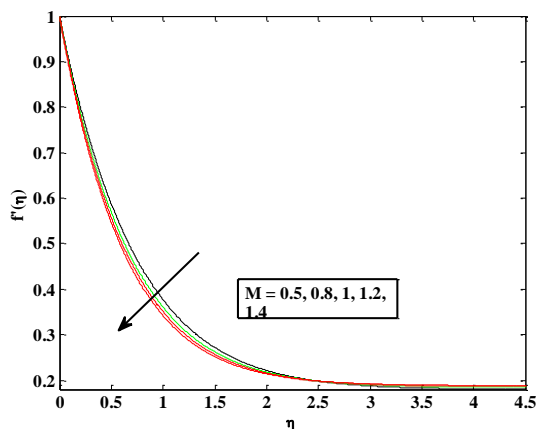


Figure-3: Effect of M on velocity

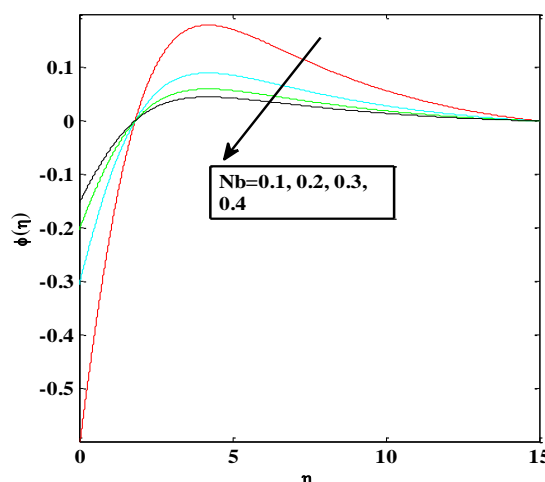


Figure-4: Effect of Nb on concentration

I.

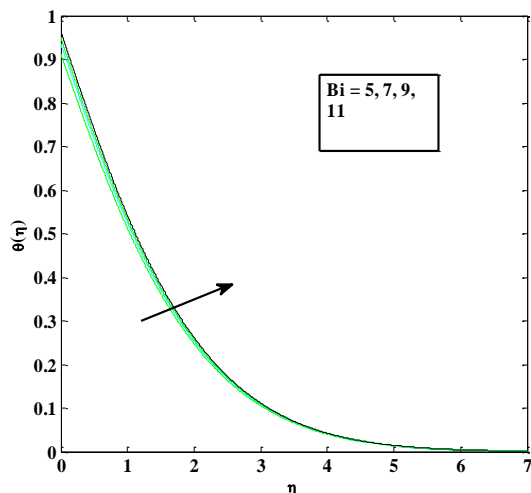


Figure-5: Effect of **Bi** on temperature

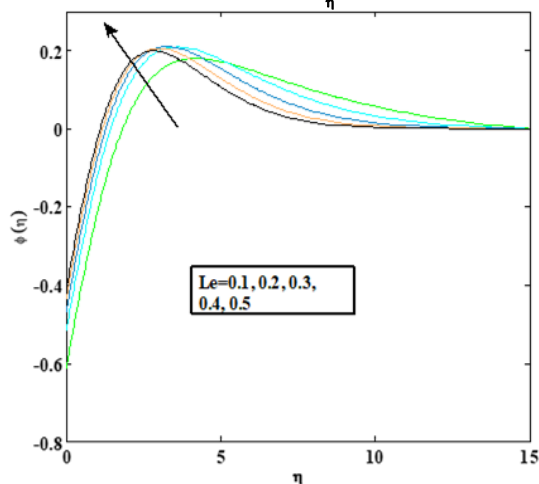


Figure-6: Effect of **Le** on concentration

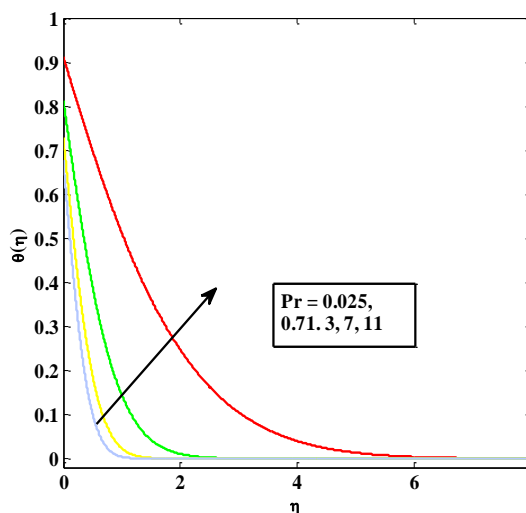


Fig .7 demonstrates the influence of Lewis number on concentration profile. Ratio of species diffusivity to thermal diffusivity is denoted by the Lewis number Le . Increase values of Le species diffusivity larger than thermal diffusivity as result concentration profile increases. Fig. 8 illustrates the influence of Prandtl number Pr on temperature profile. The ratio of momentum diffusivity to thermal diffusivity is the Prandtl number. An increase in the Prandtl number reduces the thickness of the thermal boundary layer.

Fig.9 depicted the impact of permeable parameter λ on velocity curve. As size of the pores rises with growing values permeable parameter as a result the velocity of the fluid is uplift. Fig.10 shows the influence of Thermophoresis

parameter Nt on concentration curve. It indicates the movement of the fluid particles through a fluid under the effect of temperature gradient, so that the fluid particles move from hot zone to cold zone as a result concentration of the fluid increases.

Figure-7: Effect of **Pr** on temperature

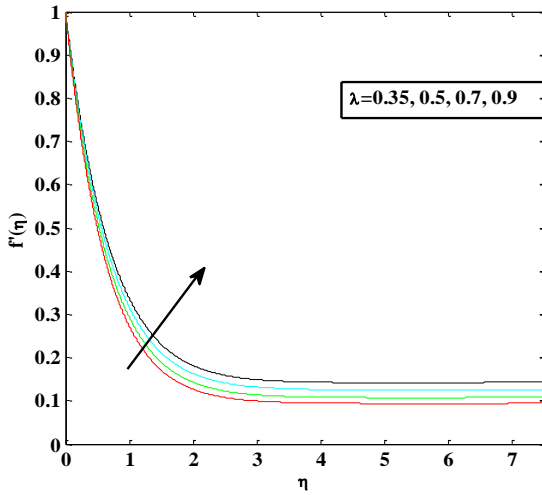


Figure-8: Effect of λ on velocity

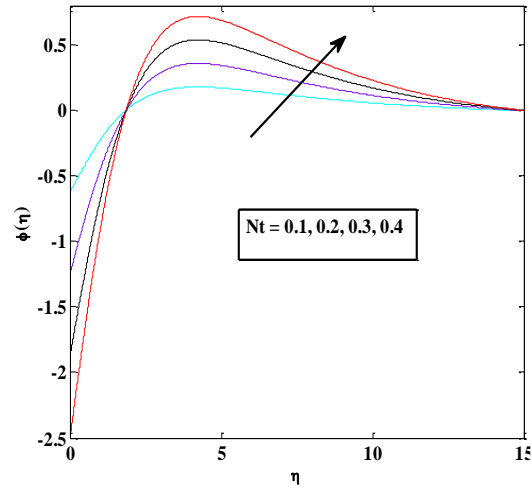


Figure-9: Effect of Nt on concentration

The effects of the most important factors on skin-friction, the rate of temperature transports, and the rate of mass transports are also shown in Table.1

Table I: Numerical values of skin-friction coefficient, rate of heat and mass transfer coefficient for variation of $A, M, Pr, Nt, Nb, Le, \lambda, Bi, Cf, Nu_x, Sh_x$.

A	M	Pr	Nt	Nb	Le	λ	Bi	$-Cf$	$-Nu_x$	Sh_x
0.2								1.124723	0.437428	0.437428
0.4								0.927773	0.482356	0.482356
0.6								0.682591	0.520818	0.520818
	0.5							1.124723	0.437428	0.437428
	0.8							1.205664	0.431729	0.431729
	1.0							1.257002	0.428215	0.428215
		0.02						1.124723	0.083755	0.083755
		0.71						1.114723	0.437428	0.437428
		1						1.086423	0.936415	0.936415
			0.1					1.098723	0.437428	0.437428
			0.2					1.124563	0.436928	0.873855
			0.3					1.144983	0.436427	1.309281
				0.1				1.124723	0.437428	0.437428
				0.2				1.124723	0.435824	0.532467
				0.3				1.124723	0.421897	0.985232
					0.1			1.026322	0.437428	0.437428
					0.2			0.983022	0.436986	0.436986
					0.3			0.966225	0.436593	0.436593
						0		1.076823	0.445125	0.445125
						0.3		1.214038	0.423321	0.423321
						0.5		1.296371	0.410705	0.410705
							5	1.083220	0.437428	0.437428
							7	1.102447	0.448628	0.448628
							9	1.111320	0.455102	0.455102

Table 2: Comparison of skin-friction coefficient results for different values of A .

A	Ch.Janaiah[16]	Present Values
0.1	0.9588412405	1.202635
0.2	0.9052341045	1.124723
0.5	0.6533901124	0.810815
2.0	2.0095542375	2.049775
3.0	4.6822357889	4.832505

CONCLUSIONS:

In the present paper mainly concentrated on the influence of porous medium, velocity ratio and convective heating parameter on steady, incompressible nanofluid flow through a non-linear stretching sheet. Using a numerical Keller - box technique, the main flow governing equations are resolved. The numerical outcomes for the concentration, temperature, and velocity profiles for the various parameters are plotted graphically and thoroughly discussed. The primary conclusions of this investigation are.

- The velocity profiles are declines by the increasing magnetic parameter and raise by growing values of Velocity ratio and Permeable parameter.
- The Velocity ratio parameter, prandtl number, and Biotnuber constant all make the local Sherwood number go up.
- The temperature distribution flattens out as the Prandtl number increases.
- For increasing permeable parameter values, the magnitude of the skin friction parameter increases while the rates of heat and mass transfer decrease.

REFERENCES

1. S.U.S. Choi, Enhancing Thermal Conductivity of Fluids with Nanoparticles, ASME, USA, 1995.
2. J. Buongiorno, Convective transport in nanofluids, ASME J. Heat Tran. 128 (2006) 240–250
3. M. Ramzan, M. Bilal, Time dependent MHD nano-second grade fluid flow induced by permeable vertical sheet with mixed convection and thermal radiation, PLoS One 10 (5) (2015) e0124929. doi: 10.1371/journal.pone.0124929
4. S.O. Adesanya, J.A. Faladeb, S. Jangilic, O.A. Bg, Irreversibility analysis for reactive third-grade fluid flow and heat transfer with convective wall cooling, Alexan. Eng. J. 56 (1) (2017) 153–160. <https://doi.org/10.1016/j.aej.2016.09.017>
5. A.K. Pandey, M. Kumar, Natural convection and thermal radiation influence on nanofluid flow over a stretching cylinder in a porous medium with viscous dissipation, Alexan. Eng. J. 56 (1) (2017) 55–62.
6. M. Bilal, M. Sagheer, S. Hussain, Three dimensional mhd upper-convected maxwell nanofluid flow with nonlinear radiative heat flux, Alexan. Eng. J. 57 (2018) 1917–1925. <https://doi.org/10.1016/j.aej.2017.03.039>
7. A. Shahzada, R. Ali, M. Hussain, M. Kamran, Unsteady axisymmetric flow and heat transfer over time-dependent radially stretching sheet, Alexan. Eng. J. 56 (1) (2017) 35–41. DOI.10.1016/j.aej.2016.08.030
8. M. Ramzan, M. Bilal, J.D. Chung, Radiative flow of Powell-Eyring magneto nanofluid over a stretching cylinder with chemical reaction and double stratification near a stagnation point, PLoS One 12 (1) (2017) e0170790 .
<https://doi.org/10.1371/journal.pone.0170790>
9. H.R. Ashorynejad, M. Sheikholeslami, I. Pop, D.D. Ganji, Nanofluid flow and heat transfer due to a stretching cylinder in the presence of magnetic field, Heat Mass Tran. 49 (2013) 427–436.
10. A.M. Rashad, S. Abbasbandy, A.J. Chamkha, Non-darcy natural convection from a vertical cylinder embedded in a thermally stratified and nanofluid saturated porous media, J. Heat Tran. 136 (2014) 022503–1–9.
DOI:10.1115/1.4025559
11. M. Satya Prasad, N. V. Swamy Naidu, and R. Srinivasa Raju, Numrical analysis of Nanofluid on Stagnation flow past a Stretching sheet in the presence of MHD ,convective heating and Double diffusive effects. J. Nanofluids 9, 346 (2021). doi:10.1166/jon.2022.1871

12. K. V. B. Rajakumar, V. S. R. Pavan Kumar, K. S. Balamurugan, and V. Bharat Kumar, Viscous dissipation and radiation absorption effect on unsteady MHD free convective fluid flow past an inclined porous with chemical reaction. *Mathematical Modelling of Engineering Problems* 7, 160 (2020). DOI:10.1002/htj.22739
13. M. Anil Kumar, Y. Dharmendar Reddy, V. Srinivasa Rao, and B. Shankar Goud, Chemical reaction impact on MHD natural convective flow through porous medium past an exponentially stretching sheet in presence of heat source/sink and viscous dissipation. *Case Studies in Thermal Engineering* 24, 100826 (2021).
14. Y. Dharmendar Reddy, V. Srinivasa Rao, and M. Anil Kumar, effect of heat generation/absorption on MHD copper- water nanofluid flow over a non-linear stretching/shrinking sheet. *AIP Conference Proceedings* 2246, 020017 (2020).
15. W. Ibrahim and Rizwan Ul Haq, *Journal of the Brazilian Society of Mechanical Sciences and Engineering* 38, 1155 (2016).
16. Ch. Janaiah and G. Upender Reddy, Numerical analysis of nanofluid on stagnation flow past a stretching sheet in the presence of MHD ,convective heating Double diffusive effects. *Journal of Nanofluids* Vol. 11, pp. 728–736, 202.